Available online at www.sciencedirect.com
ScienceDirect
Trans. Nonferrous Met. Soc. China 27(2017) 2529−2538
Transactions of Nonferrous Metals Society of China
www.tnmsc.cn

Characterization of A390 aluminum alloy produced at different slow shot speeds using vacuum assisted high pressure die casting

Wen-bo YU[1,2], Zi-hao YUAN[1,2], Zhi-peng GUO[1,2], Shou-mei XIONG[1,2]

1. School of Materials Science and Engineering, Tsinghua University, Beijing 100084, China;
2. Key Laboratory for Advanced Materials Processing Technology, Ministry of Education, Tsinghua University, Beijing 100084, China

Received 11 August 2016; accepted 13 March 2017

Abstract: The effects of vacuum assistance on the microstructure and mechanical properties of high pressure die cast A390 alloy at different slow shot speeds were evaluated. Plate-shaped specimens of hypereutectic A390 aluminum alloy were produced on a TOYO BD−350V5 cold chamber die casting machine incorporated with a self-improved TOYO vacuum system. According to the results, the vacuum pressure inside the die cavity increased linearly with the increasing slow shot speed at the beginning of mold filling. Meanwhile, tensile properties of vacuum die castings were deteriorated by the porosity content. In addition, the average primary silicon size decreased from 23 to 14 μm when the slow shot speed increased from 0.05 to 0.2 m/s, which has a binary functional relationship with the slow shot speed. After heat treatment, microstructural morphologies revealed that needle-shaped and thin-flaked eutectic silicon particles became rounded while Al_2Cu dissolved into α(Al) matrix. Furthermore, the fractography revealed that the fracture mechanism has evolved from brittle transgranular fracture to a fracture mode with many dimples after heat treatment.
Key words: A390 aluminum; shot speed; vacuum assisted high pressure die casting (VHPDC); Si distribution; tensile strength; heat treatment

1 Introduction

Due to high wear resistance, low coefficient of thermal expansion and lightweight hypereutectic aluminum−silicon alloys have been regarded as the preferred material for engine components [1−4]. After an appropriate machining and a honing procedure, surfaces with dispersed primary Si could directly provide the required tribological characteristics for a proper operation of the engine without the need of iron liners [5]. For example, hypereutectic A390 aluminum−silicon alloy (~17% Si) has been used in Chevrolet Vega engine block castings produced using low pressure die casting in the 1970s [6].

Considerable work has been carried out on the relationship between the microstructure and the tribological property of hypereutectic aluminum−silicon alloys. These investigations suggested that higher wear resistance could be obtained through uniformly fining and dispersing silicon particles [5−9]. Hence, different methods have been adopted for the size reduction of primary silicon particles. Thereby, chemical modification using rare-earth metals has been widely used [10−12]. Alternatively, physical methods such as semisolid rheo-casting [13], squeeze-casting [14], intensive melt shearing [15] and rapid solidification [16] have also been used. Compared to these methods, high pressure die casting (HPDC) belongs to the most cost effective near-net-shape manufacturing process. Indeed, during HPDC, the fast solidification rate in die cavity could reduce the externally solidified crystals (ESCs, as primary silicon) size [17,18]. YAMAGATA et al [17] also reported primary silicon particles which have nucleated when the melt was poured into the shot sleeve prior to the injection process while aluminum dendrites and eutectic silicon particles nucleated in the die cavity. Furthermore, it has been proved that the formation of ESCs in the shot sleeve strongly depends on the slow shot speed as it can affect the flow behavior and solidification condition of the molten metal in the shot sleeve before the high speed injection takes

Foundation item: Project (51775297) supported by the National Natural Science Foundation of China; Project (2015M580093) supported by the China Postdoctoral Science Foundation
Corresponding author: Shou-mei XIONG; Tel: +86-10-62773793; E-mail: smxiong@tsinghua.edu.cn
DOI: 10.1016/S1003-6326(17)60281-4

place [19−21]. From this point of view, it should be possible to control the quantity and size of primary silicon particles by modifying the slow shot speed of plunger in the shot sleeve.

The morphology of the eutectic silicon particles is generally needle-like or plate-like, which produces stress concentrations detrimental to the mechanical properties. Therefore, it is often necessary to modify their morphologies through heat treatment. Recently, it has been observed that lowering atmospheric pressure in the shot sleeve and die cavity in HPDC could minimize the porosity of the castings for the subsequent heat treatment processing [22,23]. It was revealed that the subsequent application of treatment could increase the casting strength without the blistering risk [24]. KASPRZAK et al [25] have investigated Al−17%Si−4.5%Cu−0.5%Mg based alloy subjected to T1, T5 and T6 treatments. According to their results, the application of T6 treatment resulted in the highest hardness (HRB ~85) regardless of the initial microstructure refinement.

Based on the above research discussion, the present investigation focused on the effect of different slow shot speeds on porosity and size of primary silicon particles in "plate-shape" castings. Furthermore, the influence of the heat treatment on the mechanical performance of A390 specimen was also discussed.

2 Experimental

2.1 Casting details and microstructure observation

According to the chemical analysis by ICP (Inductively Coupled Plasma), the composition of A390 alloy is listed in Table 1. The die casting experiment was conducted on a TOYO350 cold-chamber HPDC machine equipped with a self-improved TOYO vacuum system, as shown in Fig. 1.

Table 1 Chemical composition of experimental A390 cylinder liner alloy (mass fraction, %)

Si	Cu	Mg	Fe	Ti	P	Al
17.51	4.12	0.43	0.28	0.06	0.06	Bal.

During the casting experiment, the vacuum system was launched when the plunger tip moved to the 110 mm position in the shot sleeve. Subsequently, the plunger continued to move at different slow shot speeds (0.05, 0.10, 0.15 and 0.2 m/s) until the 270 mm position was reached. More details about this process are presented in Table 2.

The die cast component including three tensile test bars (diameter at the center was 6.4 mm) and one plate sample (thickness was 2.5 mm) was given in Fig. 2(a). During the casting procedure, a vacuum gauge (vacuum

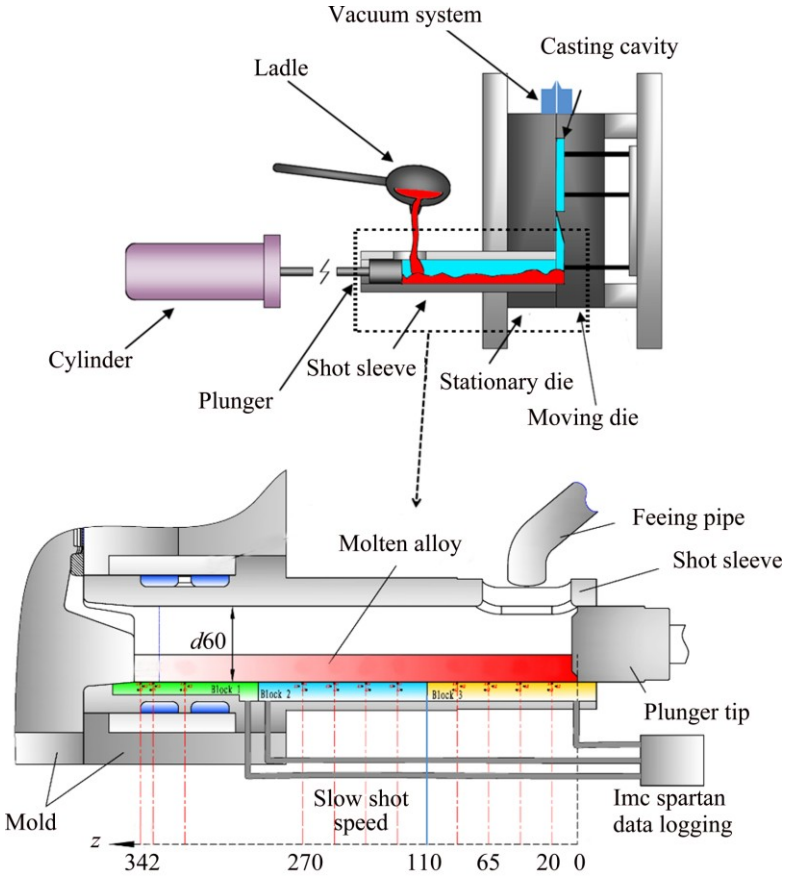

Fig. 1 Schematic of vacuum assisted HPDC process and details about shot sleeve (unit: mm)

Table 2 Details of HPDC process parameters

Parameter	Value
Pouring temperature/°C	730
Mold temperature/°C	120
Vacuum position/mm	110
Plunger moving distance/mm	425
Fast shot position/mm	270
Fast shot plunger velocity/(m·s^{-1})	1.50
Casting pressure/MPa	78

1 in Fig. 2) was inserted in the die. The dispersion of primary silicon particles on cross sections of the specimen was observed from chilled layer to the center of the metallographic (marked as A in Fig. 2(a)). Moreover, in order to quantify the volume distribution of silicon (primary and eutectic) and Al_2Cu from the chilled layer to the center, layers of 0.2 mm were gradually removed before polishing, followed by SEM observations and X-ray diffraction (D8 diffractometer, Cu K_α radiation Bruker, Germany). This procedure was repeated down to 1.2 mm depth from the top surface. XRD data were refined using the Materials Analysis Using Diffraction (MAUD) software to extract the volume content of different phases [26]. In addition, contents of primary silicon particles in different layers were quantitatively analyzed from Micro-image Analysis & Process image analysis software. At least, three micrographs were analyzed for each measurement.

2.2 Heat treatment and mechanical properties measurements

The samples were heat-treated under T6 procedure with a solution treatment at 470 °C for 30 min and an aging treatment at 168 °C for 24 h. Five specimens for each condition were used to measure the tensile properties. Tensile tests were carried out by an electronic universal testing machine and the loading rate was 1 mm/min. Elongation was obtained by a knife-edge extensometer fixed in the range of gauge length. Four tensile specimens (Fig. 2(c)) were tested, and the average value of the results was then used to evaluate their ultra-tensile strength (UTS) and elongation. The tensile test was conducted under ambient temperature (20 °C). Finally, the evolution of the microstructure before and after the T6 treatment was observed and discussed.

3 Results and discussion

3.1 Vacuum effect

The cross sectional micrographs of specimens cast at different slow shot speeds are given in Fig. 3. Like the previous report about the vacuum effect on AZ91D alloy [27−29], very low content of porosity can be found in these produced castings using assisted vacuum. The vacuum conduction was applied once the plunger reached the 110 mm position, as shown in Fig. 2. Lower slow shot speed allowed more time to perform vacuum execution. Herein, less porosity could be found in the specimen cast with lower slow shot speed [26]. Furthermore, the densities of the produced castings were measured using the Archimedes principle. The casting density decreased from (2.6±0.12) to (2.4±0.21) g/cm^3 with increasing slow shot speed from 0.05 to 0.20 m/s. This also confirmed that lower slow shot speed allowed more time to perform vacuum execution and reduce the porosities in castings.

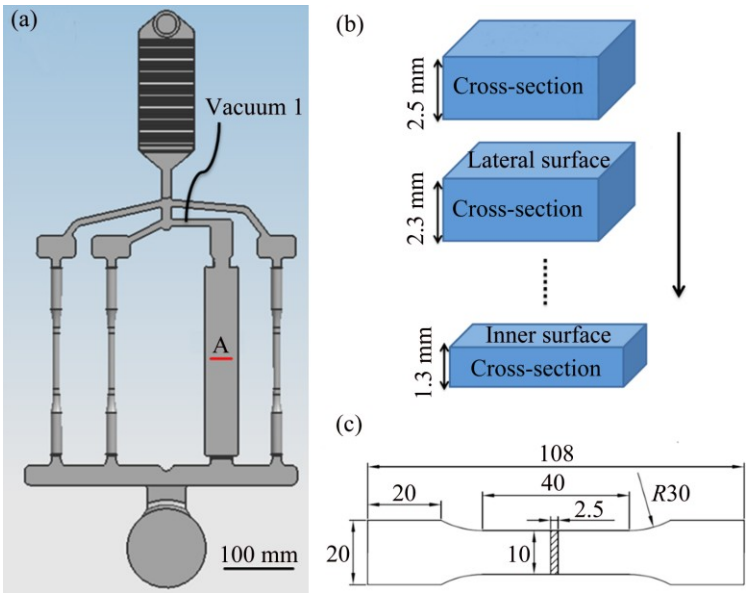

Fig. 2 Configuration of specific casting including three tensile test bars with diameter at center of 6.4 mm and one plate sample with thickness of 2.5 mm (a), observed surface from chilled layer to center (b) and tensile specimen (c) (unit: mm)

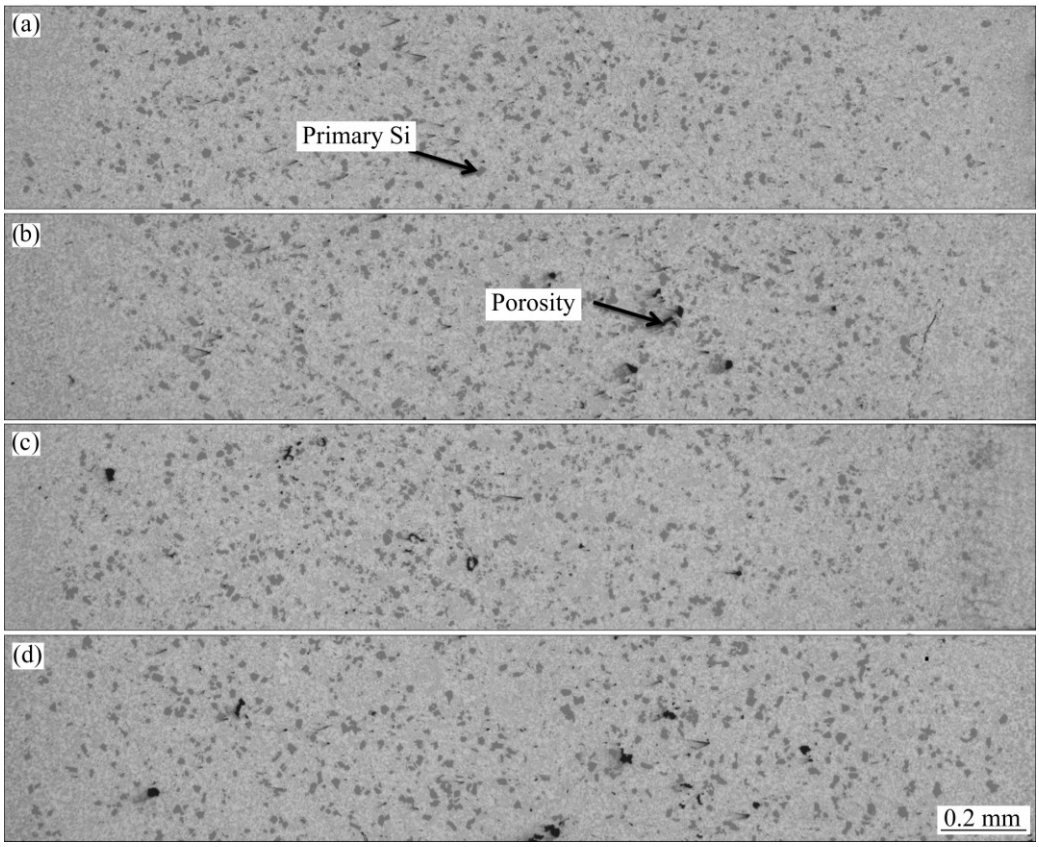

Fig. 3 Typical micrographs obtained from middle of section in 2.5 mm specimens produced at slow shot speeds of 0.05 m/s (a), 0.10 m/s (b), 0.15 m/s (c) and 0.20 m/s (d)

The variations of the measured vacuum pressure and cylinder pressure during the vacuum die casting processes at slow shot speeds of 0.05 and 0.20 m/s are given in Fig. 4(a), where t is the vacuum time in the die cavity at the beginning of mold filling. It is clear that an increase in the vacuum time resulted in the decrease of the vacuum pressure in the die cavity at the beginning of mold filling. The vacuum pressures in the die cavity at the beginning of mold filling under different slow shot speeds are illustrated in Fig. 4(b). High vacuum levels of nearly 5 kPa could be achieved in the die cavity at the beginning of mold filling under the slow shot speed of 0.05 m/s. An increase in the slow shot speed leads to a linear increase in the vacuum pressure, which is given by the well fitted linear curve.

3.2 Distribution of primary and eutectic silicon

Rietveld refinement of the XRD data using MAUD software is given in Fig. 5(a). The well-fitted curves indicated that the fitting procedure was well done. The variations in volume content of silicon (primary and eutectic) and Al_2Cu on different planes from the chilled layer to the inner side are depicted in Fig. 5(b). Under slow shot speeds of 0.05 and 0.2 m/s, both curves almost have the same trend. In the chilled layer, the silicon content is about 11%. This value is close to the silicon content at eutectic point in aluminum−silicon phase diagram, which confirms that the silicon presents as eutectic component in the surface zone. With increasing the depth, the silicon contents increased linearly and reached 18% at about 0.85 mm followed with a plateau until the specimen center. This should be attributed to the increasing primary silicon contents from the surface to the center area, which is given in Fig. 5(c). In contrast, the Al_2Cu contents decreased from the chilled surface to the specimen center. When the molten liquid met the relative cold die cavity, the fast cooling rate could shift the eutectic point. This effect resulted in higher Al_2Cu content in the chilled layer [30]. Finally, the eutectic silicon content can be extracted by subtracting the primary silicon content (Fig. 5(c)) from the total silicon content obtained from the XRD refinement results (Fig. 5(b)), as shown in Fig. 5(d). The difference between two curves revealed that more primary silicon could precipitate by decreasing the slow shot speed.

Figure 6 presents the morphologies of silicon particles and α(Al) grains in four samples at the depth of 0.4 mm from chilled layer. The common points are that the primary Si particles are dispersed uniformly in the aluminum matrix and the eutectic Si particles are

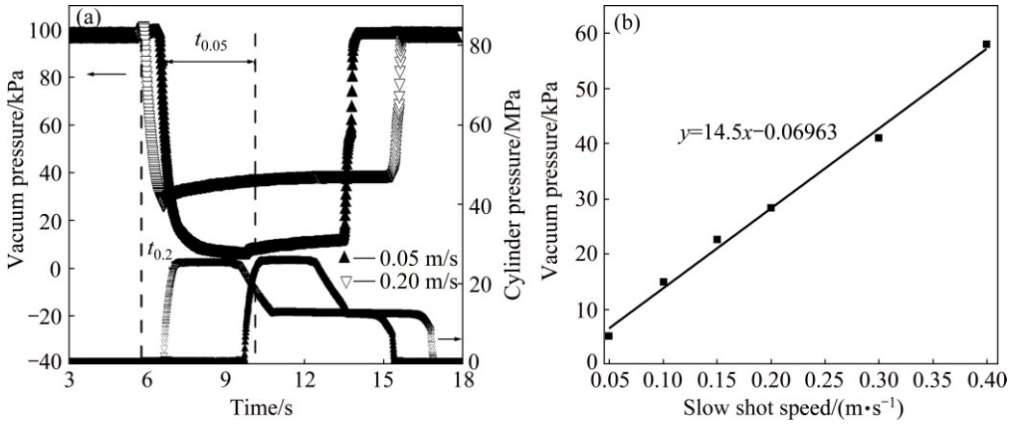

Fig. 4 Measured vacuum pressure and cylinder pressure variations vs plunger moving time at slow shot speeds of 0.05 and 0.20 m/s (a), and vacuum pressure in die cavity at beginning of mold filling vs slow shot speeds (b)

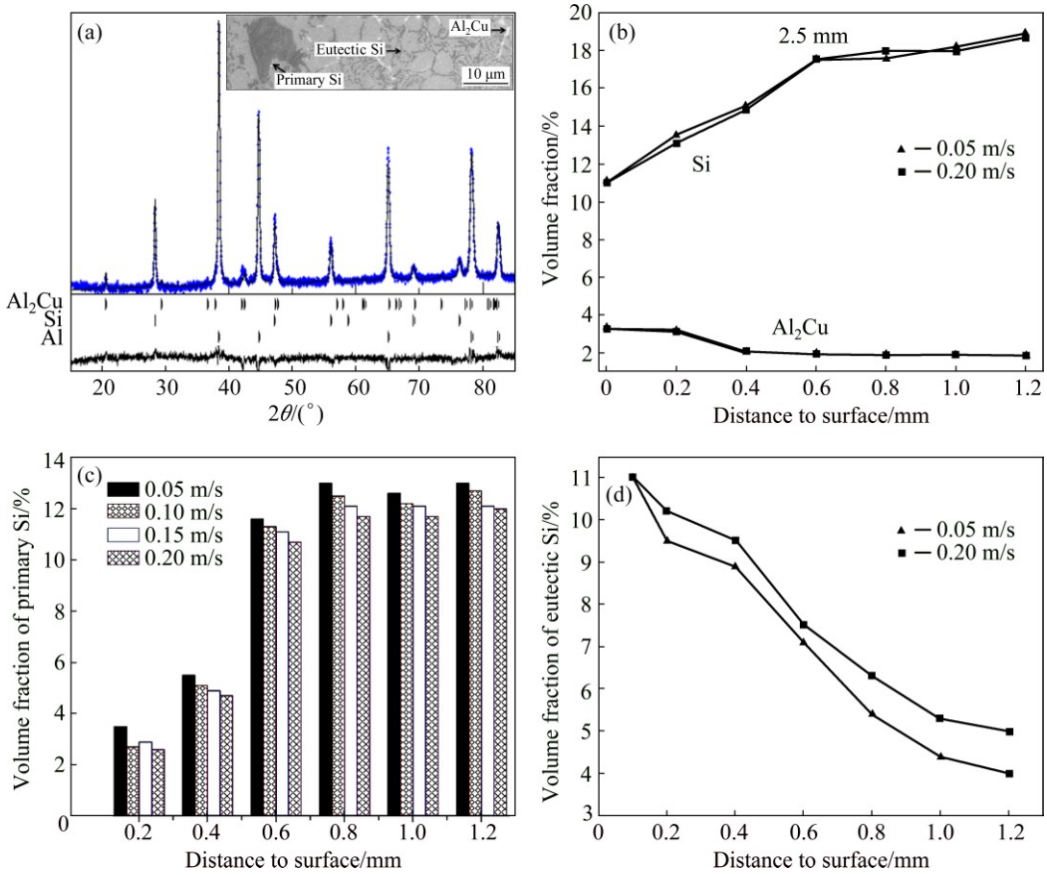

Fig. 5 Rietveld refinements on A390 specimen cast at 0.05 m/s with corresponding microstructural morphology (The eutectic silicon and Al_2Cu phases are distributed along the α(Al) grain boundaries) (a), silicon (primary and eutectic) and Al_2Cu volume fractions on different planes from top surface (b), quantity primary silicon on different planes at different slow shot speeds (c), and distribution of eutectic silicon (d)

distributed along the α(Al) grain boundaries. The difference among these samples lies in the size of primary silicon and α(Al), especially for α(Al). This should be attributed to the residence time of molten metal in shot sleeve. This behavior has also been proved in our previous work on AM60B magnesium alloy. Lower slow shot speed in shot sleeve favored the growth of α-magnesium [31].

According to the requirement of the industrial practice of engine block manufacturing, a primary Si size of approximately 20 μm is regarded as one of the acceptance criteria to meet the cylinder bore surface wear resistance requirements [17]. Herein, the size distribution of primary silicon particles from Fig. 6 was determined and given in Fig. 7. Figure 7 revealed that the primary silicon size decreased with increasing the slow

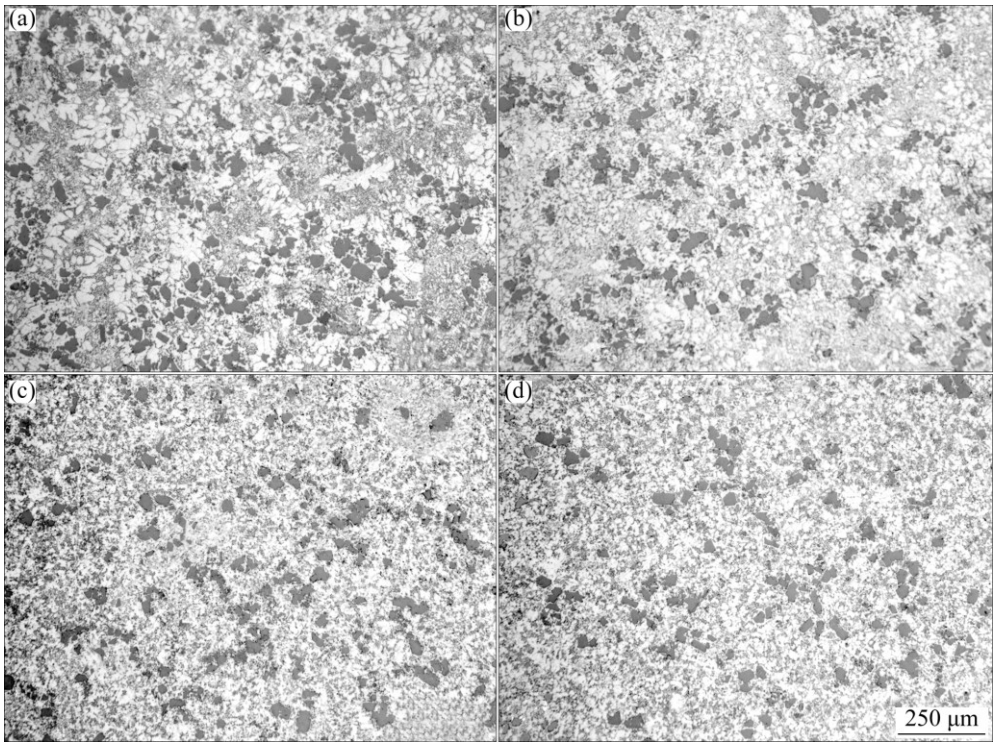

Fig. 6 Optical micrographs of planes at 0.4 mm depth in specimens produced at slow shot speeds of 0.05 m/s (a), 0.10 m/s (b), 0.15 m/s (c) and 0.20 m/s (d), showing morphologies of silicon particles and α(Al) grains

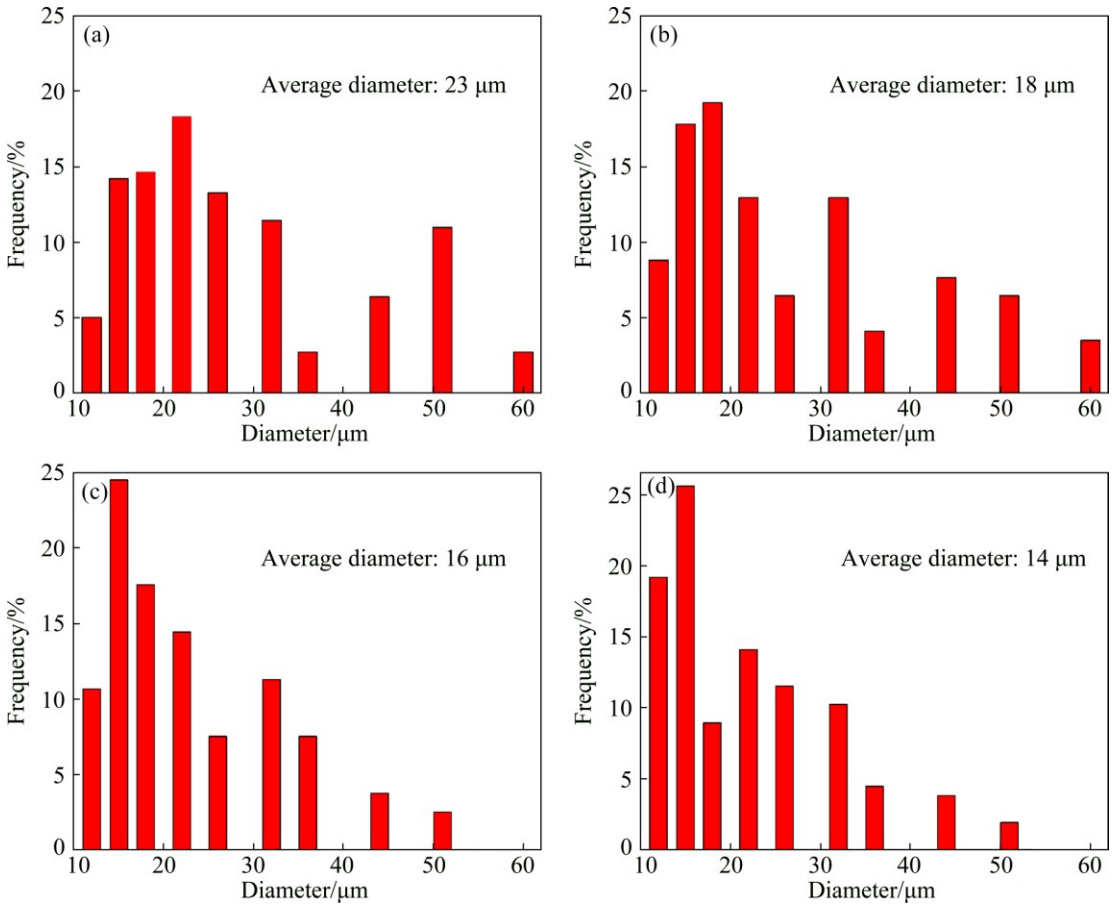

Fig. 7 Size distribution of primary silicon particles in planes at 0.4 mm depth in specimens produced at slow shot speeds of 0.05 m/s (a), 0.10 m/s (b), 0.15 m/s (c) and 0.20 m/s (d)

shot speed. Furthermore, Fig. 8 shows that the primary silicon size has a binary functional relationship with slow shot speed. Anyway, the average primary silicon size is lower than 25 μm, which suggests these castings could meet the cylinder bore surface wear resistance requirements.

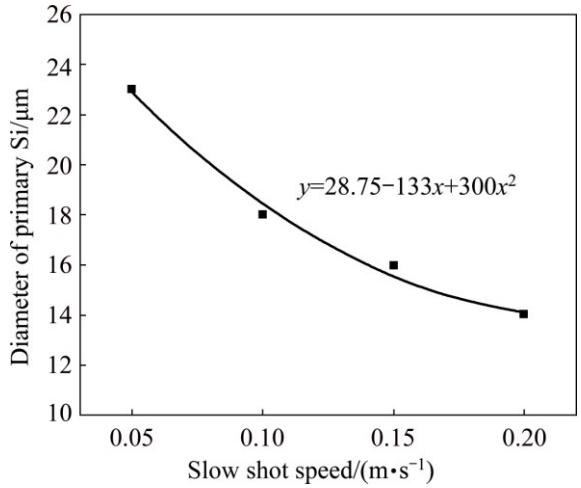

Fig. 8 Primary silicon size vs slow shot speed

3.3 Evolution of tensile strength

The variations of tensile strength respected with different slow shot speeds are presented in Fig. 9(a). Due to the porosity resulted from the less evacuated time, as shown in Fig. 3, tensile strength decreased with increasing the slow shot speed. Heat treatment had a little effect on tensile strength since no remarkable difference was observed between the untreated and treated samples. In contrast, the elongations at the fracture were strongly improved from 0.3% to 0.75% after the heat treatment, as can be seen from the pieces of plates cast at 0.05 m/s in Fig. 9(b). These results are in agreement with results of the artificial aging of Al−Si−Cu−Mg casting alloys reported by SJÖLANDER and SEIFEDDINE [32]. They pointed out that the microstructure refinement had a small influence on the yield strength as long as the solution treatment parameters were adjusted to achieve the complete dissolution of intermetallic phases and homogenization. However, the elongation at the fracture was strongly improved by increasing the microstructure refinement level.

The microstructural evolution of the cast specimen before and after heat treatment is revealed in Figs. 10(a) and (b). It was clear that most of Al_2Cu phase was dissolved into α(Al) [33]. At the same time, the long interconnected eutectic silicon particles along grain boundaries became isolated and more uniformly distributed. These changes were also confirmed in Figs. 10(c) and (d), wherein the surfaces were etched using a solution of 0.5% HF and 99.5% H_2O (volume fraction) during 30 s. Compared with the long strip-like interconnected eutectic silicon along aluminum grain boundaries shown in Fig. 10(c), the round eutectic silicon particles uniformly dispersed as the matrix in shown in Fig. 10(d). According the previous reports, the eutectic silicon particles with a needle-shape and thin-flake morphology could transform into a round morphology after heat treatment. This modification of the eutectic silicon particles has a very significant enhancement effect on ductility in hypoeutectic alloys [25]. Before heat treatment, the brittle transgranular fracture in Al matrix and cleavage fracture in primary silicon was found, which can be seen in Fig. 10(e). In contrast, many dimples were produced on the fracture surface after heat treatment (Fig. 10(f)), which could optimize the elongation of the cast specimens [34].

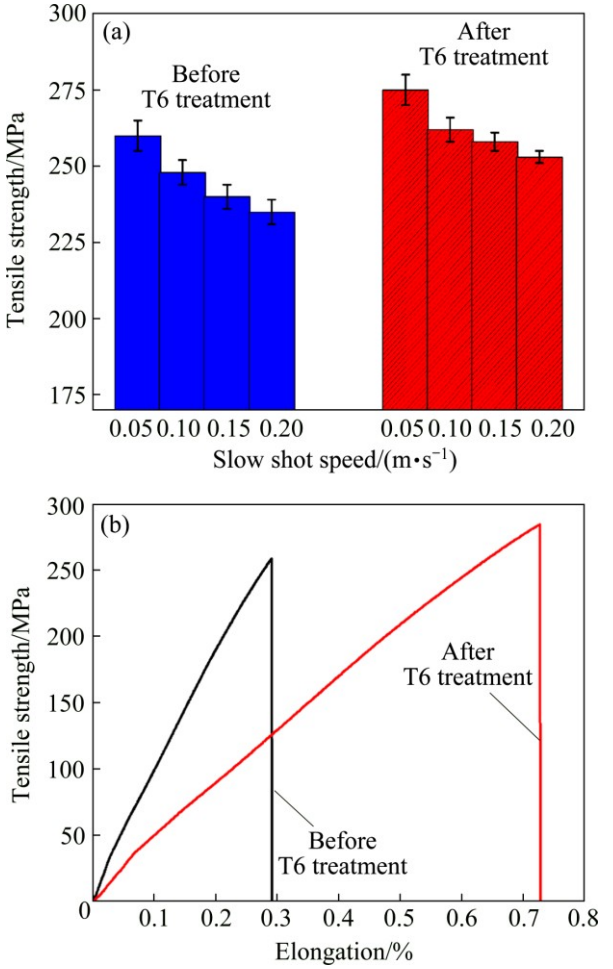

Fig. 9 Tensile strengths of 2.5 mm piece plates cast at different slow speeds before and after T6 treatment (a), and tensile strength−elongation curves of 2.5 mm piece plates cast at 0.05 m/s before and after T6 treatment (b)

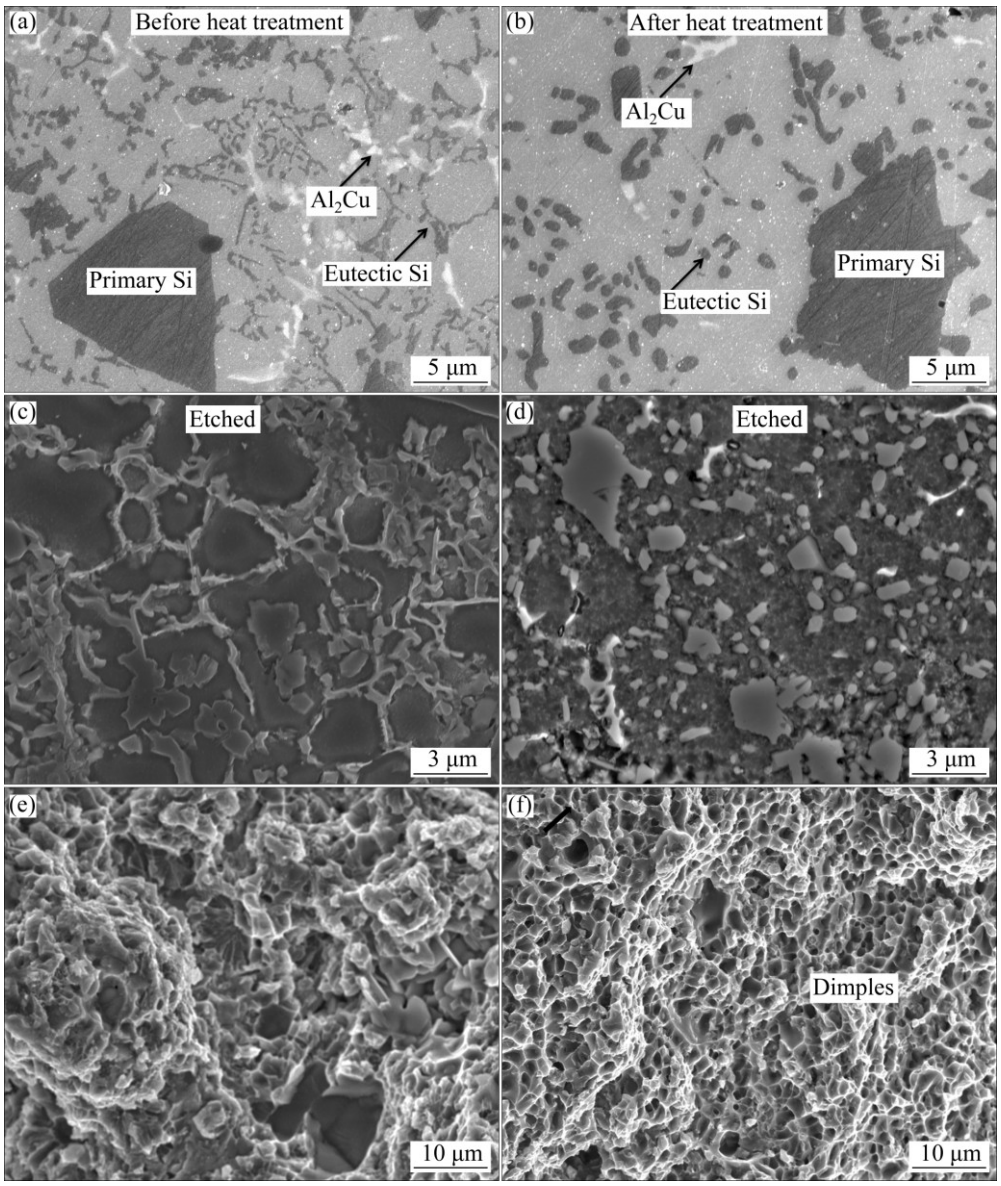

Fig. 10 Microstructures of polished surface of 2.5 mm piece plates cast at 0.05 m/s before and after T6 treatment: (a, b) Un-etched; (c, d) Etched; (e, f) Fracture surface

4 Conclusions

1) Under different slow shot plunger speeds (0.05, 0.10, 0.15 and 0.20 m/s) in vacuum assisted high pressure die casting (VHPDC) process, 2.5 mm plate specimens were produced with hypereutectic A390 aluminum alloy.

2) With increasing the slow shot speed, the vacuum pressure in the die cavity at the beginning of mold filling increased following a linear curve. The porosities in the castings appeared with increasing the slow shot speed from 0.15 m/s.

3) The average size of primary silicon decreased from 23 to 14 μm with slow shot speeds increased from 0.05 to 0.20 m/s. The primary silicon volume increased linearly and reached 12% at 0.85 mm. After that, the content of primary silicon kept steadily down to the center area. In addition, the primary silicon size has a binary functional relationship with the slow shot speed.

4) After T6 treatment, microstructural morphologies revealed that needle-shaped and thin-flaked eutectic silicon became rounded and Al_2Cu was dissolved into α(Al) matrix. After T6 treatment, this brittle transgranular fracture turned into a fracture mode with many dimples.

References

[1] LASA L, RODRIGUEZ-IBABE J. Wear behaviour of eutectic and

hypereutectic Al−Si−Cu−Mg casting alloys tested against a composite brake pad [J]. Materials Science and Engineering A, 2003, 363: 193−202.

[2] WANG Jun, GUO Zhi-peng, XIONG Shou-mei. Characterization of the morphology of primary silicon particles using synchrotron X-ray tomography [J]. Materials Characterization, 2017, 123: 354−359.

[3] YAMAGATA H. The science and technology of materials in automotive engines [M]. Cambridge: Woodhead Publishing Limited, 2005: 40−95.

[4] ARSHA A G, JAYAKUMAR E, RAJAN T P D. Design and fabrication of functionally graded in-situ aluminium composites for automotive pistons [J]. Materials & Design, 2015, 88: 1201−1209.

[5] JADOON A, MUFTI R. Tribological behaviour of alternate hypereutectic Al−Si alloys with different antiwear additives [J]. Tribology Materials, Surfaces & Interfaces, 2010, 4: 61−73.

[6] JORSTAD J L. The hypereutectic aluminum−silicon alloy used to cast the Vega engine block[J]. Modern Casting, 1971, 60: 59−64.

[7] WANG Feng, LIU Hui-min, MA Ya-jun, JIN Yuan-sheng. Effect of Si content on the dry sliding wear properties of spray-deposited Al−Si alloy [J]. Materials & Design, 2004, 25: 163−166.

[8] CHANDRASHEKHARAIAH T, KORI S. Effect of grain refinement and modification on the dry sliding wear behaviour of eutectic Al−Si alloys [J]. Tribology International, 2009, 42: 59−65.

[9] WANG Feng, MA Ya-jun, ZHANG Zheng-ye, CUI Xiao-hao, JIN Yuan-sheng. A comparison of the sliding wear behavior of a hypereutectic Al−Si alloy prepared by spray-deposition and conventional casting methods [J]. Wear, 2004, 256: 342−345.

[10] POURBAHARI B, EMAMY M. Effects of La intermetallics on the structure and tensile properties of thin section gravity die-cast A357 Al alloy [J]. Materials & Design, 2016, 94: 111−120.

[11] LI Qing-lin, XIA Tian-dong, LAN Ye-feng, LI Peng-fei, FAN Lu. Effects of rare earth Er addition on microstructure and mechanical properties of hypereutectic Al−20%Si alloy [J]. Materials Science and Engineering A, 2013, 588: 97−102.

[12] CHEN Chong, LIU Zhong-xia, REN bo, WANG Ming-xing, WENG Yong-gang, LIU Zhi-yong. Influences of complex modification of P and RE on microstructure and mechanical properties of hypereutectic Al−20Si alloy [J]. Transactions of Nonferrous Metals Society of China, 2007, 17: 301−306.

[13] JUNG H K, KIM H G, KANG C G. A study on quantitative formability assessment of rheological materials based on the microstructural characterization with a moderate control of the process [J]. Journal of Materials Processing Technology, 2007, 182: 220−228.

[14] CHA Guo-ji, LI Jian-guo, XIONG Shou-mei, HAN Zhi-qiang. Fracture behaviors of A390 aluminum cylinder liner alloys under static loading [J]. Journal of Alloys and Compounds, 2013, 550: 370−379.

[15] ZHANG Z, LI H T, STONE I C. Refinement of primary Si in hypereutectic Al−Si alloys by intensive melt shearing [J]. Materials Science and Engineering, 2011, 27: 1−6.

[16] PARK W W, YOU B S, KIM N J. Microstructure and mechanical properties of rapidly solidified Al−Si−Fe−X base alloys [J]. Materials & Design, 1996, 17: 255−259.

[17] YAMAGATA H, KASPRZAK W, ANIOLEK M, KURITA H, SOKOLOWSKI J. The effect of average cooling rates on the microstructure of the Al−20%Si high pressure die casting alloy used for monolithic cylinder blocks [J]. Journal of Materials Processing Technology, 2008, 203: 333−341.

[18] HU Zu-qi, WAN li, LU Shun-lin, ZHU Peng, WU Shen-sen. Research on the microstructure, fatigue and corrosion behavior of permanent mold and die cast aluminum alloy [J]. Materials & Design, 2014, 55: 353−360.

[19] LAUKLI H, GRACIOTTI A, LOHNE O, GJESTLAND H, SANNES S. High pressure die casting of aluminium and magnesium alloys—Grain structure and segregation characteristics [D]. Trondheim: Norwegian University of Science and Technology, 2002: 45.

[20] WU Meng-wu, XIONG Shou-mei. Microstructure characteristics of the eutectics of die cast AM60B magnesium alloy [J]. Journal of Materials Science & Technology, 2011, 27: 1150−1156.

[21] YU Wen-bo, CAO Yong-you, LI Xiao-bo, GUO Zhi-peng, XIONG Shou-mei. Determination of interfacial heat transfer behavior at the metal/shot sleeve of high pressure die casting process of AZ91D alloy [J]. Journal of Materials Science & Technology, 2017, 33: 52−58.

[22] SAKAMOTO T, KIRA K, KAMBE H. Development of automotive suspension part by high vacuum die casting [J]. Journal of Japan Foundry Engineering Society, 2004, 76: 283−288.

[23] YU Wen-bo, ZHAO Hong-bin, WANG Lei, GUO Zhi-peng, XIONG Shou-mei. The influence of T6 treatment on fracture behavior of hypereutectic Al−Si HPDC casting alloy [J]. Journal of Alloys and Compounds, 2018, 731: 444−451.

[24] KASPRZAK W, YAMAGATA H, ANIOLEK M, KURITA H. Energy efficient heat treatments for hypereutectic Al−Si engine blocks made using vacuum high pressure die-casting [J]. Journal of Materials Engineering and Performance, 2010, 20: 120−132.

[25] KASPRZAK W, KURITA H, BIRSAN G, AMIRKHIZ B S. Hardness control of Al−Si HPDC casting alloy via microstructure refinement and tempering parameters [J]. Materials & Design, 2016, 103: 365−376.

[26] LUTTEROTTI L, MATTHIESAND S, WENK H. MAUD: A friendly Java program for material analysis using diffraction [J]. IUCr: Newsletter of the CPD, 1999, 21: 14−15.

[27] LI Xiao-bo, XIONG Shou-mei, GUO Zhi-peng. Improved mechanical properties in vacuum-assist high-pressure die casting of AZ91D alloy [J]. Journal of Materials Processing Technology, 2016, 231: 1−7.

[28] WANG Qing-liang, XIONG Shou-mei. Vacuum assisted high-pressure die casting of AZ91D magnesium alloy at different slow shot speeds [J]. Transactions of Nonferrous Metals Society of China, 2014, 24: 3051−3059.

[29] WANG Qing-liang, XIONG Shou-mei. Effect of multi-step slow shot speed on microstructure of vacuum die cast AZ91D magnesium alloy [J]. Transactions of Nonferrous Metals Society of China, 2015, 25: 375−380.

[30] RHINES F N. Phase diagrams in metallurgy: Their development and application [M]. New York: McGraw-Hill, 1956: 68−100.

[31] WANG Bai-shu, XIONG shou-mei. Effects of shot speed and biscuit thickness on externally solidified crystals of high-pressure diet cast AM60B magnesium alloy [J]. Transactions of Nonferrous Metals Society of China, 2011, 21: 767−772.

[32] SJÖLANDER E, SEIFEDDINE S. Artificial ageing of Al−Si−Cu−Mg casting alloys [J]. Materials Science and Engineering A, 2011, 528: 7402−7409.

[33] CHOI S W, CHO H S, KANG C S, KUMAI S. Precipitation dependence of thermal properties for Al−Si−Mg−Cu−(Ti) alloy with various heat treatment [J]. Journal of Alloys and Compounds, 2015, 647: 1091−1097.

[34] CHOI S W, KIM Y M, LEE K M. The effects of cooling rate and heat treatment on mechanical and thermal characteristics of Al−Si−Cu−Mg foundry alloys [J]. Journal of Alloys and Compounds, 2014, 617: 654−659.

不同慢压射速度高真空压铸制备 A390 铝合金及其性能表征

于文波[1,2]，袁梓豪[1,2]，郭志鹏[1,2]，熊守美[1,2]

1. 清华大学 材料科学与工程学院，北京 100084；
2. 清华大学 先进成形制造教育部重点实验室，北京 100084

摘　要：对真空辅助不同慢压射速度条件下制备的 A390 高硅铝合金铸件组织及力学性能进行研究。在装备自行改进 TOYO 真空系统的 TOYO BD−350V5 型冷室压铸机上制备片状 A390 压铸件。结果表明，型腔中的真空度与初始充模阶段慢压射速度呈线性关系。拉伸试验结果表明, 试样的拉伸强度随试样内部的孔洞含量升高而降低。另外，当慢压射速度从 0.05 m/s 增大到 0.2 m/s 时, 初晶 Si 尺寸由 23 μm 降低到 14 μm，初晶 Si 的平均尺寸与慢压射速度存在二元次数关系。 经热处理后，初始铸态 α(Al)边界上的 Al_2Cu 因融入 Al 基体中而大幅减少，并且针状或带状共晶 Si 球化。断裂形貌表明, 断裂形式由热处理前的脆性沿晶断裂转变为热处理后的含有大量韧窝的韧性穿晶断裂。

关键词：A390 铝合金；压射速度；真空压铸；Si 元素分布；拉伸强度；热处理

(Edited by Wei-ping CHEN)